Glutaraldehyde-assisted crosslinking in regenerated cellulose films toward high dielectric and mechanical properties

Menghang Gao
Southwest Jiaotong University
Xu Xie
Southwest Jiaotong University
Ting Huang
Southwest Jiaotong University
Nan Zhang
Southwest Jiaotong University
Yong Wang (yongwang1976@163.com)
Southwest Jiaotong University

Research Article

Keywords: Cellulose, Crosslinking, Dielectric properties, Mechanical properties

Posted Date: April 5th, 2022

DOI: https://doi.org/10.21203/rs.3.rs-1329529/v1

Glutaraldehyde-assisted crosslinking in regenerated cellulose films toward high dielectric and mechanical properties

Meng-hang Gao, Xu Xie, Ting Huang, Nan Zhang*, Yong Wang*

Key Laboratory of Advanced Technologies of Materials (Ministry of Education), School of Materials Science & Engineering, Southwest Jiaotong University, Chengdu, 610031, China

Abstract: Developing the green dielectric materials satisfies the requirement of the sustainable development of society and economics. In this work, glutaraldehyde (GA)-assisted crosslinking strategy was developed to prepare the crosslinked regenerated cellulose (CRC) films, and the effects of different crosslinking methods, including crosslinking steps, concentration of GA solution and crosslinking time, on dielectric and mechanical properties of the CRC films were systematically investigated. Microstructure and morphology characterizations show that compared with the common RC films, the CRC films show apparently reduced defects and enhanced intermolecular interaction. At GA concentration of 6 vol% and crosslinking time of 30 min, the CRC film shows the lowest dielectric loss (0.03 at 1000 Hz, 92.3% smaller than RC film) and the highest breakdown strength (336.55 MV m^{-1}, 364.3% higher than RC film), and simultaneously, the film shows the high tensile strength of 76.8 MPa and excellent tensile modulus of 6.08 GPa, about 240.9% and 104% higher than those of RC film, respectively. This work provides new insight in tailoring the dielectric and mechanical properties of the cellulose films through constructing the crosslinking structure, which is of great significance for the fabrication of the high-performance cellulose-based dielectric materials.

Keywords: Cellulose; Crosslinking; Dielectric properties; Mechanical properties

1. Introduction

Recently, with the rapid development of social economy, energy problems are increasingly serious (Yu et al. 2017). The preparation +of green, environmentally friendly, and renewable energy storage materials is of great significance to the construction of a sustainable society. Among energy storage devices, dielectric capacitors with the advantages of high-power density, fast charging and discharging speed, etc., have gradually obtained the widespread attention (Liu et al. 2020; Zhang et al. 2020). As the main materials of dielectric capacitors, dielectric materials

* Corresponding author:
E-mail: yongwang1976@swjtu.edu.cn (Y. Wang), sanyenan@163.com (N. Zhang)

with good dielectric properties have a wide range of applications in many civil and military fields, such as active vibration control (Sarban et al. 2011; Zhao et al. 2019), aerospace (Li et al. 2015; Li et al. 2018) and bioelectronics applications (Joyce et al. 2013), etc.

As we all know, traditional dielectric polymers are often synthetic polymers based on petrochemical resources, such as polypropylene (PP) (Yuan et al. 2020), poly(vinylidene fluoride) (PVDF) (Prateek et al. 2016), poly(methyl methacrylate) (PMMA) (Zheng and Wong 2003), polyimide (PI) (Kaltenbrunner et al. 2013), etc. For example, Liu SH et al (Liu et al. 2014) prepared the PVDF composites containing high aspect ratio surface-hydroxylated $Ba_{0.6}Sr_{0.4}TiO_3$ nanotubes (BST-NT) and found that the composite with 10 vol% BST-NT showed a dielectric constant of 48.2 at a frequency of 1 kHz, which was 6.1 times higher than that of the pure PVDF (7.9). However, these synthetic polymers have the common characteristics, namely, they are non-biodegradable and non-renewable, and the fabrication of such dielectric materials usually leads to serious environmental pollutions, such as the widely existed “plastic microparticles” in water (Wang et al. 2020). With the depletion of resources and increasing environmental problems, obviously, it is of great significance to develop the green polymers-based dielectric materials.

Cellulose, as one of the most abundant materials in nature, has good biocompatibility, non-toxicity, biodegradability and recyclability (Seddiqi et al. 2021). In the microstructure of cellulose, 1,4-glycosidic bonds link β-D-glucopyranosyl groups to form cellulose molecular chains (Croll and Schroeder 2004). Due to the regular molecular chain structure and the large number of hydroxyl groups, there are many intermolecular and intramolecular hydrogen bonding interactions, which endow cellulose with promising physicochemical performances, such as good mechanical performances, high solubility resistance and good chemical resistance, etc (Djahedi et al. 2016). Cellulose is one of the most promising green materials, and the effective use of cellulose resources has become a research hotspot in the fields of chemistry, chemical engineering and materials science. To data, various structural and/or functional materials based on cellulose have been developed, and some of them have gained commercial applications (Moon et al. 2011).

Developing the cellulose-based dielectric materials have also attracted much attention of researchers (Zhao et al. 2021). Among these researches, most of them were focused on incorporating nanoparticles into cellulose to prepare the dielectric composites, and these nanoparticles are various, including titanium dioxide (TiO_2) (Madusanka et al. 2016; Tao et al.

2019), magnetite (Arantes et al. 2019), barium titanate ($BaTiO_3$) (Morsi et al. 2019), alumina (Al_2O_3) (Yin et al. 2021)，MXene (He et al. 2020), Boron Nitride (Lao et al. 2018a), graphene oxide (GO) (Wang et al. 2018), montmorillonite (Madusanka et al. 2017), carbon nanotubes (Zeng et al. 2016), etc. For example, Zhang CG et al (Zhang et al. 2019) prepared regenerated cellulose (RC)/$BaTiO_3$ nanocomposite films and found that the composite film with 2 vol % $BaTiO_3$ exhibited an ultrahigh discharged energy density of 13.14 J cm^{-3} at a breakdown strength of 370 MV m^{-1}. Lao JP et al (Lao et al. 2018b) prepared cellulose/boron nitride nanosheets (BNNS) composites, and the breakdown strength was greatly improved and the composites with 10 wt% BNNS exhibited the energy storage density of 4.1 J cm^{-3} and breakdown voltage of 370 MV m^{-1}.

Although the incorporation of nanoparticles leads to the great enhancement of dielectric constant of the cellulose-based dielectric composite, the apparent increase of dielectric loss is usually unavoidable. Furthermore, because of the poor melt-processing ability, most of the cellulose-based composites reported in literature have been prepared through solution compounding processing. It is well known to all that cellulose is difficult to dissolve in common organic solvents, and the RC-based films usually have many defects, which is very unfavorable for the suppression of the intrinsic dielectric loss of the cellulose matrix (Liu et al. 2021; Zhang et al. 2016). Therefore, from a viewpoint of declaring microstructure-performance relationship, studying the dependence of dielectric properties of the cellulose-based materials on the intrinsic microstructures is of great significance. However, to date, less researches have been carried out to study the effects of molecular chain structure on the dielectric properties of the cellulose-based composites. Some researchers have pointed out that the introduction of functional groups in the molecular chains of cellulose can effectively tailor the dielectric properties (Takechi et al. 2016; Yang et al. 2018), while others investigated the dielectric performance dependence on molecular weights of cellulose (Yin et al. 2020). However, more information about the fabrication method tailoring the dielectric performances of the cellulose-based materials is still highly required.

Herein, the environmentally friendly cotton cellulose was used to prepare the RC film. During the RC film fabrication, the crosslinking reaction was introduced with the aid of glutaraldehyde (GA). Different strategies were developed to prepare the GA-crosslinked RC (CRC) films and the dielectric and mechanical properties of the two kinds of cellulose films were comparatively investigated. The results show that the crosslinking method exhibits great role in

tailoring the comprehensive performances of the CRC films. At appropriate fabrication conditions, the CRC film shows largely reduced dielectric loss, highly enhanced breakdown strength and high mechanical properties, which provides a good opportunity for further fabricating the cellulose-based dielectric composites with promising dielectric performances.

2. Experimental section

2.1 Materials

Cotton cellulose fibers with degree of polymerization (DP) of 330 was provided by Xinxiang Chemical Fiber Company. Lithium hydroxide (LiOH), urea (Urea), and GA with 50 vol% aqueous solution were provided by Shanghai Aladdin Company, China. Sulfuric acid (98%) was provided by Chengdu Kelong Chemical Reagent Factory. All these chemical reagents have analytic purity.

2.2 Preparation of the common regenerated cellulose films

The fabrication procedures of the RC film were explained in Figure 1. Cotton cellulose was immersed in 4% NaOH for 4h under stirring, then was washed to PH=7 with water. Urea and LiOH were firstly dissolved in the deionized water to prepare the alkali/urea (AU) solvent. The solvent was then cooled to -15 °C, and a certain mass of dried cellulose was added into it. The suspension was stirred at 1800 rpm for 5 min to prepare the cellulose solution with a concentration of 4 wt%. After that, the cellulose solution was centrifuged at 5000 rpm for 10 min to remove air bubbles in the solution. Subsequently, the centrifuged solution was coated on a glass plate with a spatula, and this glass plate was subsequently soaked in the 5% H_2SO_4 solution for 5 minutes. In order to prevent the film from deforming, the two sides of the film were clamped with clips. Finally, the film was washed with deionized water to remove the small molecule impurities, and then placed in an oven to be dried to obtain the RC film.

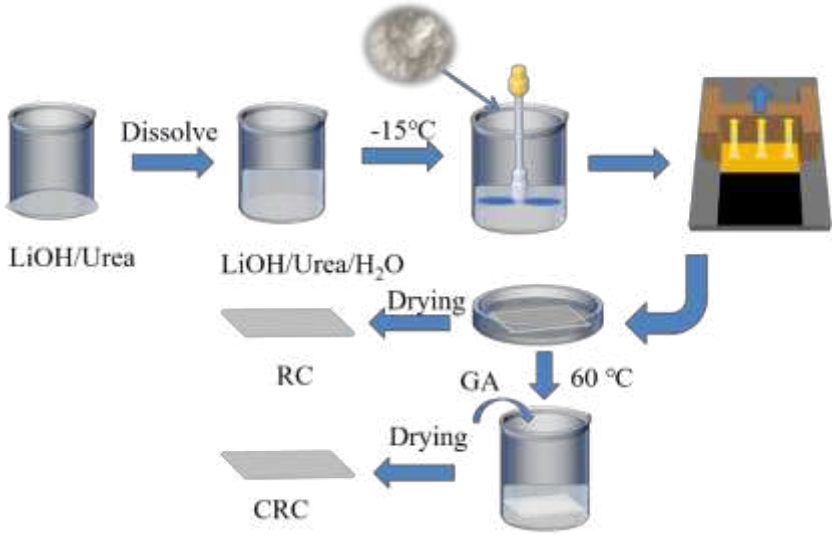

Figure 1. Schematic diagram showing the preparation procedures of the common RC and CRC films.

2.3 Preparation of the crosslinked regenerated cellulose films

The GA-assisted crosslinking of the RC films was carried out through different strategies.

The first one is crosslinking in solution. Namely, once cellulose was completely dissolved in the solvent system, 10 mL GA solution with a concentration of 2 vol% was added. After being continuously stirred for 20 min to ensure the completely crosslinking of GA, the CRC film was obtained through centrifugation, film-forming and drying steps as mentioned above. The sample notation is defined as CRC-I.

The second strategy is crosslinking before gelation. Namely, when the centrifuged solution was coated on the glass plate to obtain the film, the glass plate was immersed into the GA solution for 20 min at 60 °C, after that the glass plate was taken out and immersed into the H_2SO_4 solution for gelation. After being successively washed and dried, the CRC film was obtained. This kind of film is labelled as CRC-II.

The third strategy is crosslinking after gelation. Namely, once the RC film was obtained in the H_2SO_4 solution, it was taken out and immersed into the GA solution for 20 min at 60 °C. After that, the crosslinked RC film was taken out, washed and dried successively to obtain the target film. The sample notation was then defined as CRC-III. First, different crosslinked RC films were fabricated through changing the concentrations of GA solution (2, 4, 6, and 8 vol%) while the crosslinking reaction time was kept at 20 min, and the sample notation was named as *a*-CRC-20, where *a* represents the concentration of GA solution. Second, the crosslinking reaction time was

varied at 20, 30, 40 and 60 min and the GA concentration was kept at 6 vol%, and correspondingly, the sample notation was named as 6-CRC-*b*, where *b* represents the crosslinking reaction time. According to the literature (Aburabie et al. 2021), GA-assisted crosslinking of cellulose molecular chains can be explained in Figure 2.

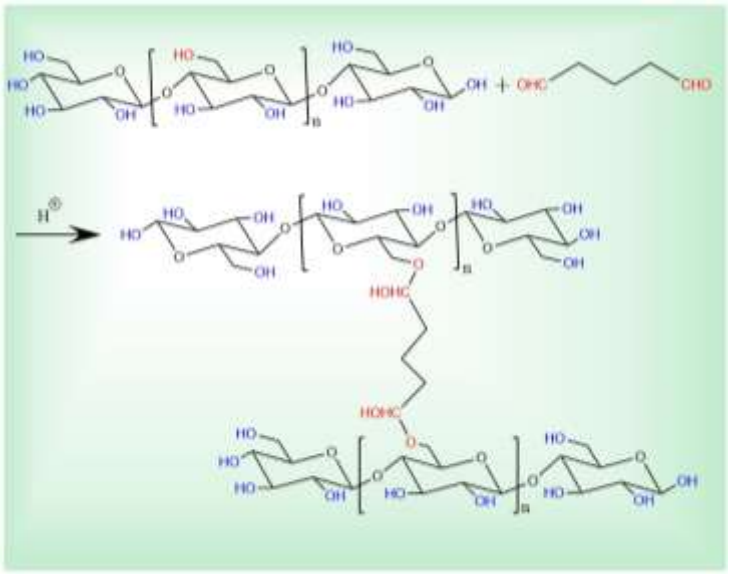

Figure 2. Chemical principle diagram of glutaraldehyde crosslinked regenerated cellulose film.

2.4 Characterization and measurements

The surface morphologies of the RC films were characterized suing a scanning electron microscope (SEM, QUANTA FEG 450, USA) at the operating voltage of 2.7 kV and current of 83 mA and an atomic force microscope (AFM, BRUKER Multimode8, Germany) *via* the contact mode. An X-ray photoelectron spectrometer (XPS, Thermo Scientific K-Alpha, America) was used to detect the chemical features of the RC and CRC films. The chemical structures of the RC and CRC films were further characterized using a Fourier transform infrared spectrometer (FTIR, BRUKER TENSOR II, Germany), and the wavenumber range was set at 400−4000 cm^{-1} with a resolution of 4 cm^{-1}. The crystalline structure of the RC films was characterized using a wide-angle X-ray diffractometer (WAXD, Panalytical Empyrean, Netherlands) with the scanning angle range of 10°−60°. The thermal stability of the cellulose films was evaluated through thermogravimetric analysis (TGA) on a G209F1 Libra (Netzsch, Germany). During the measurements, about 8 mg sample was heated from 30 °C to 800 °C at a heating rate of 10 °C min^{-1} in nitrogen atmosphere.

The optical transmittance was measured by an ultraviolet−visible spectrometer (UV−vis,

SHIMADZU, Japan). The wavelength range was set at 400−800 nm. The electrical conductivity and the dielectric property measurements were conducted on a broad frequency dielectric spectrometer, Concept 80 (Novocontrol, Germany), and the measurements were carried out at 23 °C and 220 V in the frequency range of 10^2–10^7 Hz. The dielectric breakdown strength of the sample was measured using a breakdown voltage tester (BDJC-50 KV, Beiguang Jingyi Instrument, PR China). The voltage was increased at a rate of 1.5 kV s^{-1} using an alternating current, and the highest measured voltage was 30 kV. The universal testing machine (XS(08)XT-3, Xusai, Shanghai) was used to measure the tensile properties at room temperature of 25 °C and humidity of 55%. The width of the sample was 5 mm, the gauge length was set at 35 mm, and the cross-head speed was 1 mm min^{-1}. The measurement for each kind of film was repeated for 5 times and the average value was reported.

3. Result and discussion

3.1 GA-assisted crosslinking in the regenerated cellulose film

According to the literature (Hou et al. 2019), under the acidic condition, the aldehyde groups of GA can react with the hydroxyl groups of cellulose molecular chains and thereby, GA can be the crosslinking agent of the cellulose, constructing the chemical crosslinking bonds between molecular chains of cellulose. Figure 3 shows the comparison of the surface morphologies of the RC and CRC films obtained through SEM and AFM characterizations, and the roughness parameters obtained through AFM characterizations are also provided. Here, the crosslinking reaction was introduced after gelation of cellulose in H_2SO_4 solution. Different from the relative rough surface with many holes of the common RC film (Figure 3a_1, a_2), the CRC film (Figure 3b_1, b_2) exhibits smooth surface and fewer holes. Through AFM characterizations, the roughness parameters (R_q and R_a , which represent the root-mean-square roughness and average surface roughness of the film, respectively) of the films can be obtained. As shown in Figure 3a_4 and Figure 3b_4, the CRC film shows much more homogeneous surface with lower roughness parameters (R_q of 16.7 nm and R_a of 26.9 nm) compared with the common RC sample, which shows the R_q of 54.6 nm and R_a of 42.8 nm, respectively. The above results clearly confirm that the GA-assisted crosslinking is favorable for improving the film-forming quality and reducing the

defects in the cellulose films.

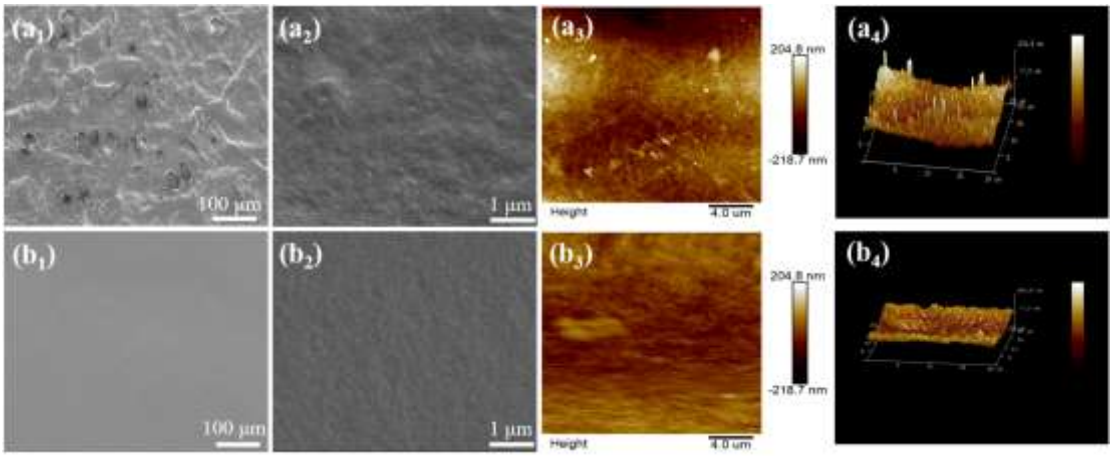

Figure 3. SEM (a_1, a_2, b_1, b_2) and AFM (a_3, a_4, b_3, b_4) images showing the surface morphologies of the RC (a_1-a_4) and CRC (b_1-b_4) films characterized at different modifications. The CRC film was obtained via crosslinking in 6 vol% GA solution for 30 min.

To better understand the effects of GA-assisted crosslinking on microstructure and intermolecular interaction of cellulose film, more characterizations were carried out. Figure 4a and Figure 4b show the C 1s spectra of the common RC and crosslinked CRC films, respectively. For the common RC film, it shows the characteristic peaks at 287.6, 286 and 284.3 eV, relating to the C=O, C-O and C-C bonds, respectively (Fras et al. 2005). The CRC film shows the completely same characteristic peaks with very small changes of peak positions. However, one can see that the CRC films show much larger peak area of C-O bonds, this clearly confirms the crosslinking of cellulose molecules by GA, leading to more C-O bonds in the CRC film. By the way, the presence of C=O bonds can be attributed to the presence of a few urea and GA molecules in the CRC film.

Figure 4c shows the FTIR spectra of the common RC and CRC films. For the common RC film, there is a strong characteristic absorption band at about 3422 cm^{-1} relating to the stretching vibration of -OH groups. While for the CRC film, the absorption band of -OH shifts to higher wavenumbers on the one hand. On the other hand, the intensity of the absorption band is apparently reduced. These changes confirm that crosslinking weakens the hydrogen bonding interaction between cellulose main chains. First, the occurrence of crosslinking consumes some hydroxy groups of cellulose molecular chains because the crosslinking occurs between the hydroxy groups of cellulose and aldehyde groups of GA (Aburabie et al. 2021). Second, the presence of GA molecules possibly increases the distance between chain segments of cellulose, reducing the probability of forming intramolecular hydrogen bonding interaction. The similar

variation trend is also observed for the characteristic absorption band at about 1630 cm^{-1} relating to the ring stretching band of glucose units (Movagharnezhad and Moghadam 2017). Furthermore, one can see that the characteristic absorption bands at 1162 cm^{-1} and 1028 cm^{-1}, which are usually attributed to the stretching vibration of C-O-C and bending vibration of C-O, respectively, becomes more resolved. This further confirms the successful crosslinking of cellulose molecules by GA (Cuba-Chiem et al. 2008).

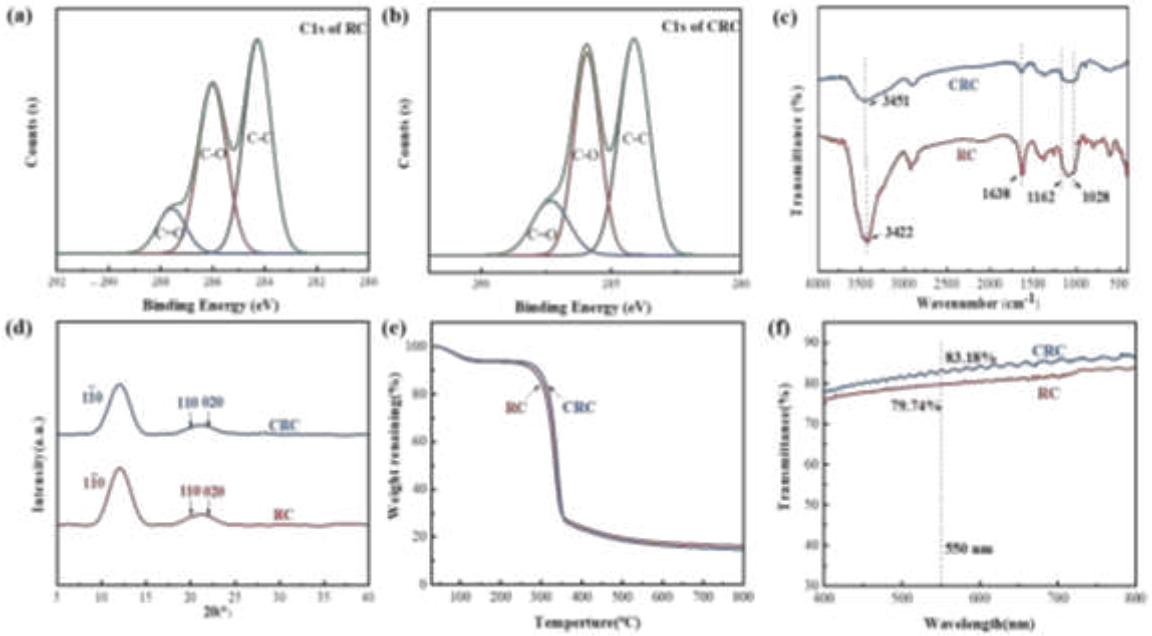

Figure 4. (a, b) XPS spectra of C 1s of the common RC and CRC films, respectively. (c) FTIR spectra, (d) WAXD profiles, (e) TGA curves and (f) transmittance of the common RC and CRC films. The CRC film was obtained via crosslinking in 6 vol% GA solution for 30 min.

Figure 4d shows the comparison of the WAXD profiles of RC and CRC films. It has been well known to all that the main crystal form of the RC film obtained by dissolution and regeneration procedures is cellulose II, which exhibits the characteristic diffraction peaks at around 12°, 20° and 22° attributed to the $(1\bar{1}0)$, (110) and (020) crystal plane respectively (French 2014). The position and intensity of characteristic peaks before and after crosslinking are basically unchanged, indicating that crosslinking has no significant influence on the crystal structure of cellulose (Hou et al. 2019).

Furthermore, the thermal stability of the RC and CRC films were also evaluated by TGA measurements, and the results are shown in Figure 4e. Compared with the RC film, which shows the thermal decomposition temperature at around 329.3 °C, the CRC film exhibits slightly

enhanced decomposition temperature at around 339.7 ℃, indicating that crosslinking facilitates the slight enhancement of the thermal stability to a certain extent. The light transmittance of the RC and CRC films are shown in Figure 4f. Here, the light transmittance was measured at wavelength range of 400-800 nm, and the ultraviolet transmittance at 550 nm is used to represent the transparency of the films. The RC film shows the transmittance of about 79.74%, while for the CRC film, the transmittance is slightly enhanced to 83.18%. The improvement of the transmittance can be attributed to the more homogenous structure with fewer holes (defects) as well as the smooth surface of the CRC film as previously confirmed by morphological characterizations. Whatever, the above results clearly show that GA-assisted crosslinking in the CRC film are successfully achieved, and the CRC film has fewer defects compared with the common RC film. This is believed to be favorable for the improvement of the dielectric and mechanical properties.

3.2 The effects of crosslinking methods on the dielectric and mechanical properties of cellulose films

Then, different crosslinking methods were used to crosslink the cellulose, and the dielectric properties were measured, so that the appropriate crosslinking method could be determined. Figure 5a–5c show the frequency dependence of dielectric constant (ε'), dielectric loss ($\tan\delta$) and comparison of the data collected at 1000 Hz, and the variations of the conductivity of the RC

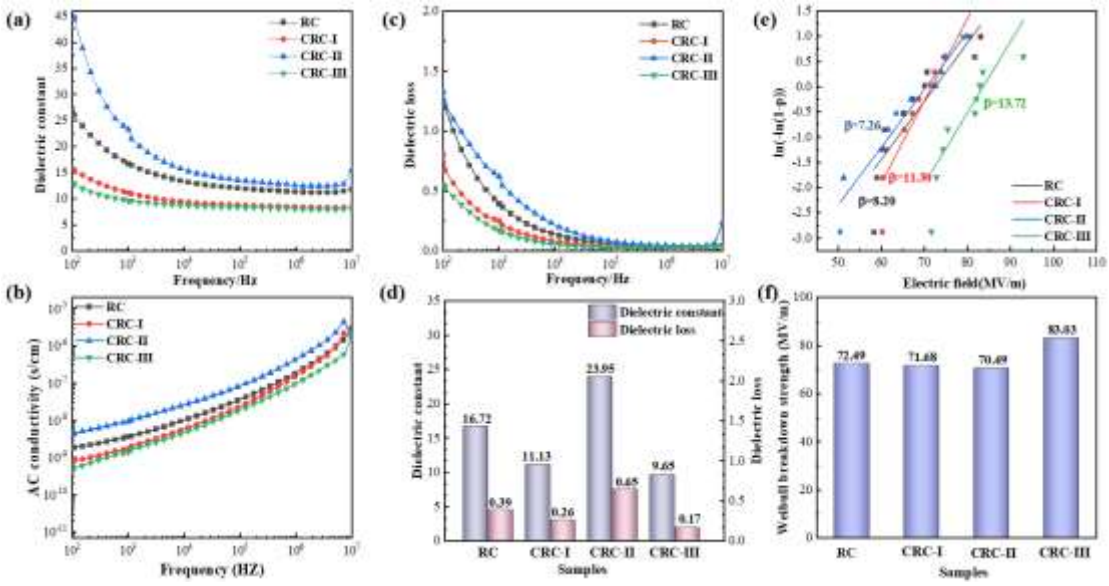

Figure 5: (a)-(d): Frequency dependence of dielectric constant, dielectric loss and conductivity of the cellulose films without and with different crosslinking methods, (e)-(f): the Weibull distribution diagram of the breakdown strength of cellulose films and the corresponding feature breakdown strength.

and CRC films are shown in Figure 5d. The effects of crosslinking on dielectric properties of the RC film are dramatic at the low frequency ranges. Generally, there are several polarization modes in polymer and/or polymer composites, such as atomic polarization, electronic polarization, dipole polarization, ionic polarization and interfacial polarization, etc. In the polymer composites, the interfacial polarization mainly determines the dielectric properties of the composites and the polarization occurs at the frequency range of 10^0–10^2 Hz, while in the polymer with polar groups, the dipole polarization exhibits the determinable role, which occurs at the larger frequency ranges compared with the polymer composites (Bonardd et al. 2019). According to Figure 5 it is deduced that the crosslinking mainly affects the dipole polarization of the cellulose film. For the common RC film, it exhibits the relatively good dielectric properties with ε' of 16.72 and $\tan\delta$ of 0.39 at frequency of 1000 Hz. Compared with the common RC film, the CRC film prepared through introducing crosslinking before gelation (CRC-II) exhibits the highest ε' and $\tan\delta$ nearly at all frequency ranges. And at frequency of 1000 Hz, ε' and $\tan\delta$ achieve 23.95 and 0.65, respectively. However, the CRC film prepared through introducing crosslinking after gelation (CRC-III) exhibits the lowest ε' and $\tan\delta$ at all frequency ranges, and in this condition, ε' and $\tan\delta$ are only 9.65 and 0.17 at 1000 Hz, much smaller than those of the common RC film. This confirms that crosslinking method has great role in tailoring the dielectric properties of the CRC film. Figure 5d shows the frequency dependence of conductivity. Compared with the common RC film, the CRC films show the similar variation trends to those of the dielectric properties.

The different variation trends of the dielectric properties are mainly related to the occurrence of the crosslinking reaction and the resultant molecular chain interaction. Generally, GA-induced crosslinking reaction occurs in the acidic condition (Aburabie et al. 2021). For the CRC-I film, the crosslinking occurred in the LiOH/Urea solvent system and in this condition, to ensure the complete dissolution of cellulose and prevent the gelation of cellulose, the added amount of GA solution was relatively small, only 10 mL and therefore, the degree of the crosslinking is relatively small. For the CRC-II film, the crosslinking reaction was introduced before gelation and in this condition, some impurities (LiOH, Urea, GA and their reaction products with H_2SO_4) might be knocked in the film during the subsequent gelation process in the H_2SO_4 solution, which possibly contribute to the polarization of the film in the electric field on the one hand. On the other hand,

283 the chemical crosslinking structure introduced by GA most likely affects the gelation of cellulose
284 in the H_2SO_4 solution. For example, the skeleton of GA molecules not only increases the distance
285 between main chains of cellulose but also enhances the rigidity of molecular chains, which reduce
286 the formation ability of hydrogen bonds between cellulose molecular chains. In other words, in the
287 CRC-II film, the molecular chains of cellulose have higher mobility and the dipole polarization
288 becomes more available. However, for the CRC-III film, after gelation in H_2SO_4, the
289 intermolecular and intramolecular hydrogen bonds already form in the gel and in this condition,
290 some of the hydroxy groups in the cellulose molecular chains have already been consumed and
291 therefore, the subsequent crosslinking reaction with GA only occurs between the free hydroxy
292 groups of cellulose and GA and in this condition, the films possibly have the highest interaction
293 among molecular chain segments. In this condition, the mobility of cellulose molecular chains is
294 greatly suppressed and consequently, the CRC-III film exhibits the low polarization effect in the
295 electrical field.

296 Figure 5e and 5f show the Weibull-distribution plots of breakdown strengths of the different
297 cellulose films and the comparison of the feature breakdown strengths. The Weibull-distribution
298 function is defined through the equation (Almalki and Nadarajah 2014):

299 $$P = 1 - \exp\left[-\left(\frac{E}{\alpha}\right)^{\beta}\right] \qquad (1)$$

300 Where P and E represent the cumulative probability of electric failure and the breakdown
301 strength obtained during the measurements, respectively. α is usually used to represent the feature
302 breakdown strength (E_{bd}) of the sample, i.e. the breakdown strength obtained at the cumulative
303 failure probability of 63.2%. β is a parameter that can be used to describe the reliability of the
304 dielectric materials and larger β indicates the higher reliability. According to equation (1), the
305 plots of $\log[-\ln(1-p)]$ versus $\log E$ can be illustrated, and then the value of α and β are
306 also obtained. The detailed data analysis can be seen in literature (Lu et al. 2019). As shown in
307 Figure 5e and 5f, the common RC film shows the breakdown strength of about 72.49 MV m^{-1}. The
308 low breakdown strength can be partially attributed to the poor film quality with many defects
309 (holes) as confirmed by morphological characterizations. It is worth noting that the film formation
310 of common RC occurs in the H_2SO_4 solution and in this condition, most of the molecular chains

311 are physically crosslinked and the role of chemical crosslinking is very small. The CRC-I and
312 CRC-II shows the similar E_{bd} to that of the common RC film. However, the CRC-III film shows
313 the highest β and the feature breakdown strength achieves 83.66 MV m^{-1}. The enhanced
314 breakdown strength can be attributed to the high quality of the film with fewer defects. This
315 indicates that the CRC-III film has high reliability and it is possibly the most appropriate one
316 among these cellulose films if they are used as the dielectric materials. Therefore, the CRC-III
317 film is selected in the following section to further declare the effects of crosslinking on dielectric
318 and mechanical properties of the CRC film.

319 Figure 6 shows the typical stress-strain curves and the corresponding mechanical property
320 parameters of the RC and CRC films obtained after different crosslinking methods. The CRC-I
321 and CRC-II films show the similar tensile strength and tensile modulus to those of the common
322 RC film, which exhibits the tensile strength and tensile modulus of 22.53 MPa and 2.98 GPa,
323 respectively, but they exhibit lower elongation at break. Among all these CRC films, the CRC-III
324 film has much higher tensile strength and tensile modulus, and the elongation at break is also
325 comparable to that of the common RC film. It has already been reported that higher mechanical
326 properties usually lead to larger breakdown strength in the electric field (Dan et al. 2019). And
327 therefore, the reason why the CRC-III film shows the highest β and E_{bd} can be partially
328 attributed to the best mechanical properties among these CRC films. Whatever, the above results
329 clearly confirm that the CRC-III film has the lowest $\tan\delta$, highest β and E_{bd}, and best
330 mechanical properties, and it has great potential as the dielectric material.
331

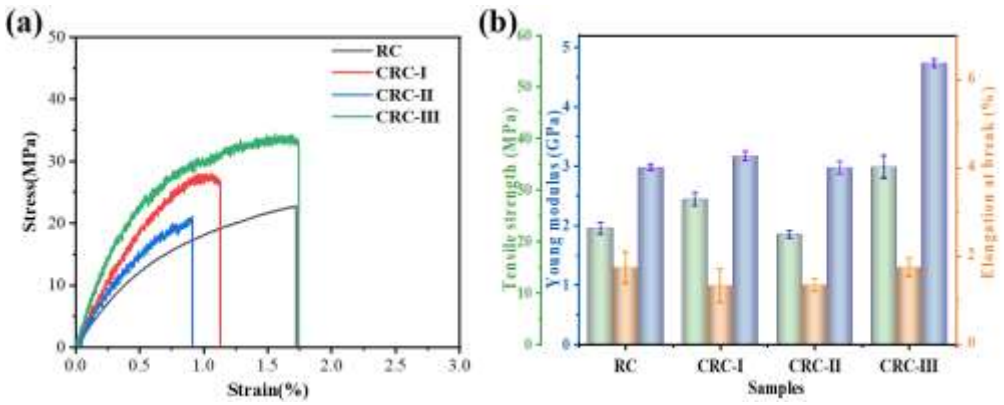

332

333 **Figure 6.** (a) Tensile stress-strain curves of crosslinking RC films with different crosslinking methods, (b)
334 comparison of the tensile properties among different membrane samples as indicated.

3.2 The effects of GA concentration on the dielectric and mechanical properties of cellulose film

As mentioned above, constructing crosslinking structure is favorable for improving the comprehensive properties of the CRC films. It is well known to all that the degree of the crosslinking is greatly dependent upon the concentration of GA solution during the crosslinking reaction. Obviously, lower GA concentration leads to smaller degree of crosslinking at the same reaction time while larger GA concentration possibly leads to excessive crosslinking in the film, which is unfavorable for the polarization of molecules in the electric filed. Most likely, there is an appropriate GA concentration for the CRC film if it is used as the dielectric material. The following section is to declare the dependence of the dielectric and mechanical properties of the CRC-III film on the GA concentration.

Figure 7 shows the dielectric properties of the CRC-III films prepared at different GA concentrations (2, 4, 6 and 8 vol%). The crosslinking reaction time was kept at 20 min. From Figure 7a-7c it can be seen that ε' and $\tan\delta$ firstly decrease with increasing GA concentrations and the lowest values are achieved at GA concentration of 6 vol%. In this condition, ε' of the 6-CRC-20 film is only 5.77 at 1000 Hz, about 65.5% lower than that of the RC film (16.72). However, it is also noticed that the $\tan\delta$ of the 6-CRC-20 film is also greatly reduced to 0.05 at 1000 Hz, about 87.2% lower than that of the RC sample. Obviously, the reduction of the $\tan\delta$ is much more apparent than that of the ε'. Further increasing GA concentration leads to higher ε' and $\tan\delta$. The variations of the dielectric properties agree well with the change of the conductivity of the films as shown in Figure 7d. At low frequency ranges, the 6-CRC-20 film shows the lowest conductivity while the 8-CRC-20 film shows the highest one. Whatever, all the CRC films show the lower conductivities compared with the RC film. As expected, increasing GA concentration leads to higher E_{bd}. Among these films, the 6-CRC-20 film has the highest E_{bd} (124.58 MV m^{-1}), which is 71.9% higher than that of the pure RC film (72.49 MV m^{-1}), while the 8-CRC-20 film has the smallest E_{bd} (58.23 MV m^{-1}), about 19.7% lower than that of RC film.

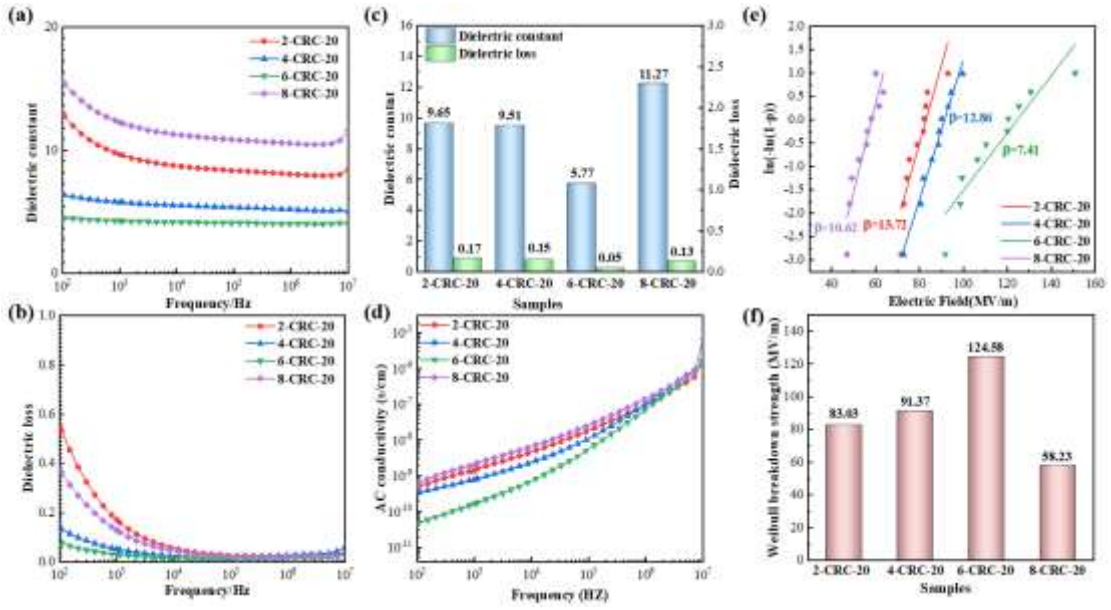

Figure 7. (a)-(d) Frequency dependence of dielectric constant, dielectric loss and conductivity of the CRC (CRC-III) films prepared at different GA concentrations, (e)-(f): the Weibull distribution diagram of the breakdown strength of these CRC films and the corresponding feature breakdown strength. The crosslinking reaction time was kept at 20 min.

The effects of GA concentration on the dielectric properties of the CRC films can be explained as follows. As mentioned above, crosslinking restricts the motion of diploes in the electric field and obviously, higher degree of crosslinking results in lower mobility of diploes, which leads to lower polarization degree of the CRC film. But higher degree of crosslinking also leads to stronger intermolecular interaction, which is favorable for the enhancement of the electric breakdown strength of the CRC film. Here, at relatively low GA concentration (2 vol%), the crosslinking reaction is relatively few in the CRC film, resulting in relatively lower degree of crosslinking. Increasing GA concentrations leads to higher degree of crosslinking in the CRC film, and therefore, ε' and $\tan\delta$ decreases while E_{bd} increases, until the minimum ε', $\tan\delta$ and the maximum E_{bd} are achieved at GA concentration of 6 vol%. However, at relatively high GA concentration (8 vol%), possibly some residual GA molecules are present in the CRC film, and these free GA molecules may contribute to the dramatic increase of ε' and $\tan\delta$. The other possibility is that at relative high crosslinking reaction rate resulted by higher GA concentration, a small quantity of water may be knocked in the CRC film and can not be easily removed during the subsequent drying treatment.

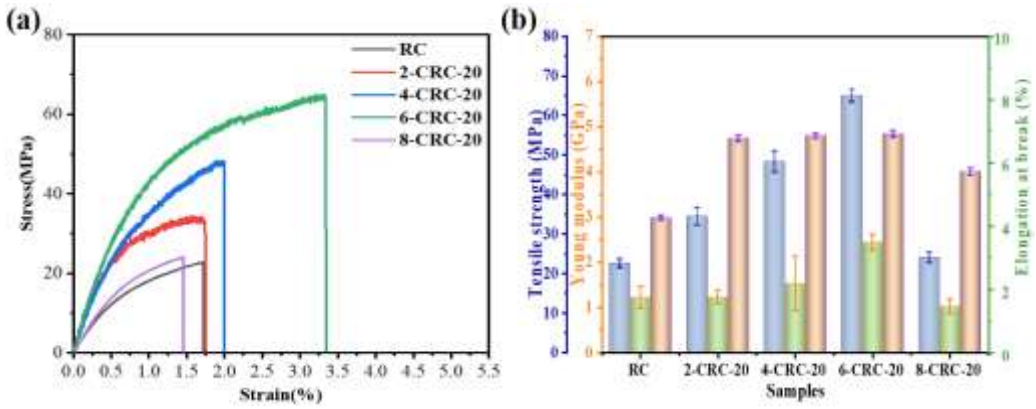

Figure 8. (a) Stress-strain curves of the common RC and the *a*-CRC-20 films and (b) the corresponding mechanical property parameters.

The effects of GA concentrations on the mechanical properties of the CRC-III films are shown in Figure 8. Among these films, the 6-CRC-20 samples shows the largest tensile strength (61.4 MPa), tensile modulus (4.80 GPa) and the tensile ductility (3.47%). Through constructing the double-network structures in the hydrogel to improve the strength and toughness has already been widely reported in literature (Zhao et al. 2016). In this work, with the increase of GA concentration, the degree of the crosslinking in the CRC films increases gradually and consequently, the enhanced intermolecular interaction leads to better strength and toughness. However, the 8-CRC-20 film exhibits worse mechanical properties, which are even lower than those of the RC film. The excessive crosslinking with extremely high crosslinking degree may greatly restricts the mobility of cellulose molecules, leading to lower tensile ductility on the one hand. On the other hand, the residual GA molecules may exhibit the plasticizing effect, leading to the reduction of both tensile strength and tensile modulus. Whatever, the above results clearly confirm that among these CRC films, the 6-CRC-20 film is possibly the most appropriate candidate as the dielectric material from a viewpoint of the relatively good comprehensive physical properties.

3.3 The effects of crosslinking reaction time on the dielectric and mechanical properties of cellulose film

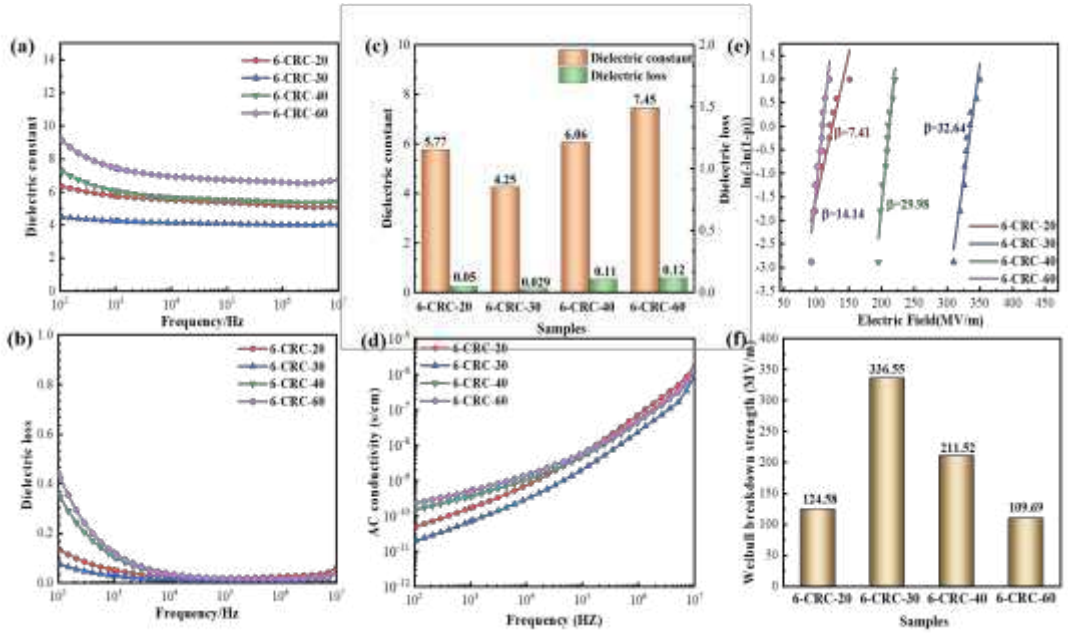

Figure 9: (a)-(d) Frequency dependence of dielectric constant, dielectric loss and conductivity of the CRC (CRC-III) films prepared at different reaction time, (e)-(f): the Weibull distribution diagram of the breakdown strength of these CRC films and the corresponding feature breakdown strength. The crosslinking reaction occurred in the 6 vol% GA solution.

The following section is then clarifying the effect of crosslinking reaction time on the dielectric and mechanical properties of the CRC-III films. According to the previous results, the concentration of GA was maintained at 6 vol% while the crosslinking reaction time was varied from 20 to 60 min. As shown in Figure 9, ε' and $\tan\delta$ tend to decrease at crosslinking time of 20 and 30 min, and the minimum values are achieved at reaction time of 30 min. Then, further increasing reaction time results in the gradual increase of the ε' and $\tan\delta$. The conductivity shows the similar variation trends with ε' and $\tan\delta$ at low frequency ranges. While the E_{bd} shows the inverse variation trend. Namely, the highest E_{bd} is achieved at reaction time of 30 min. Therefore, from a view point of dielectric properties, the 6-CRC-30 film is possibly the most appropriate candidate as dielectric material. It shows the lowest $\tan\delta$ of 0.03 at the frequency of 1000 Hz and the highest E_{bd} of 336.55 MV m^{-1}, which are about 92.3% lower and 363% higher than the $\tan\delta$ (0.39) and E_{bd} (72.49 MV m^{-1}) of the common RC film, respectively.

Similarly, the mechanical properties of the 6-CRC-*b* films were also measured, and the results are illustrated in Figure 10. Compared with the common RC film, all the 6-CRC-*b* films

show the greatly enhanced mechanical properties. Similar to the variation trend of the dielectric breakdown strength, the tensile strength and tensile modulus initially increase with increasing crosslinking reaction time, and the maximum values are achieved for the 6-CRC-30 film, which exhibits the tensile strength of 76.8 MPa and tensile modulus of 6.08 GPa. Compared with the common RC film, the tensile strength and tensile modulus of the 6-CRC-30 film are increased by 348.88% and 171.14%, respectively. However, further increasing reaction time leads to the slight reduction of both tensile strength and tensile modulus. The similar variation trends of dielectric breakdown strength and mechanical properties further confirm that there is strong relationship between them, and better mechanical properties usually ensure the higher breakdown strength of the CRC films.

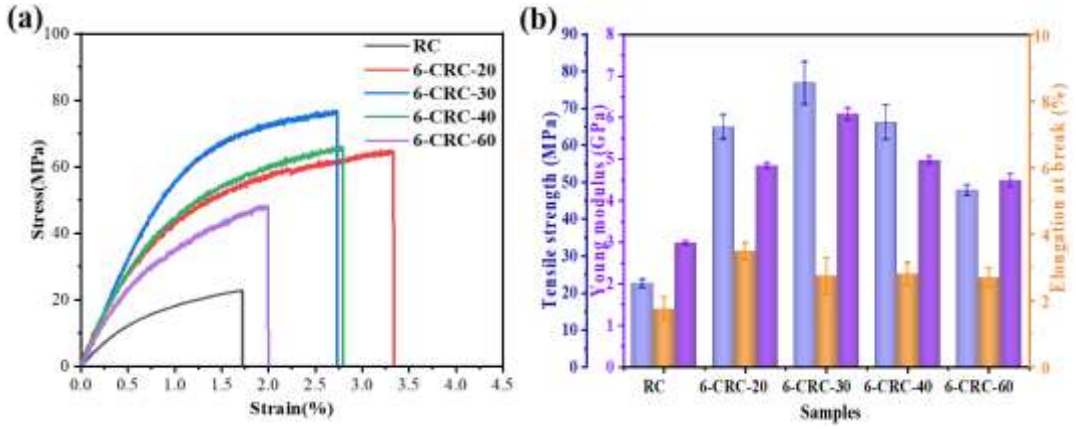

Figure 10. (a) Stress-strain curves of the common RC and the 6-CRC-*b* films and (b) the corresponding mechanical property parameters.

According to the above results, it can be clearly seen that the dielectric and mechanical properties of the CRC films are greatly dependent upon the fabrication methods. For the GA-assisted crosslinking, there are most appropriate crosslinking parameters, such as the appropriate GA concentration (6 vol%) and appropriate crosslinking time (30 min). After being crosslinked, the mobility of the chain segments is reduced, which leads to the lower degree of polarization in the electrical field, resulting in lower ε' and $\tan\delta$. Due to the enhanced mechanical properties and the reduced defects, the CRC films show enhanced E_{bd}. However, the above results also indicate at least that there is a contradiction in enhancing the ε', E_{bd} and simultaneously reducing the $\tan\delta$ in the present state. Further work is still required to further improve the

dielectric and mechanical properties of the cellulose-based materials. One possible solution is simultaneously introducing the polar groups in the molecular chains and the crosslinking structure to enhance ε' and suppress $\tan\delta$ synchronously, and the other possible solution is incorporating nanoparticles but simultaneously restricting the mobility of cellulose chains nearby the nanoparticles. The related work is being carried out in our group and will be reported in the near future.

4. Conclusion

In summary, different crosslinking methods have been developed to prepare the cellulose-based dielectric materials in this work. First, the effects of crosslinking on the morphology and microstructures of the regenerated cellulose film have been systematically investigated, and the results show that GA-assisted crosslinking improves the film-forming quality of the RC film with fewer defects. Then, the effects of crosslinking steps, the concentration of GA solution and the crosslinking time on the dielectric and mechanical properties of the CRC films have been comparatively studied. The results show that immersing cellulose hydrogel into GA solution is the most efficient way to achieve relatively good comprehensive properties. Furthermore, there are appropriate GA concentration (6 vol%) and crosslinking time (30 min), at which the CRC film exhibits relatively good dielectric properties, including the lowest $\tan\delta$ of 0.03 at frequency of 1000 Hz and the highest E_{bd} of 336.55 MV m^{-1}, and simultaneously, the tensile strength and tensile modulus achieve 76.8 MPa and 6.08 GPa, respectively. This work confirms that introducing crosslinking structure is the highly efficient way to synchronously tailor the dielectric and mechanical properties of the regenerated cellulose films, which provides significant information for the fabrication of the high-performance cellulose-based dielectric materials.

CRediT authorship contribution statement

Menghang Gao: Conceptualization, Methodology, Data curation, Formal analysis, Writing - original draft, Writing - review & editing. **Xu Xie:** Formal analysis, Investigation, Visualization. **Ting Huang:** Investigation, Discussion. **Nan Zhang:** Investigation, Discussion, Funding acquisition. **Yong Wang:** Conceptualization, Investigation, Funding acquisition, Project administration, Supervision, Writing - review & editing

Declaration of competing interest

The authors declare that they have no known competing financial interests or personal relationships that could have appeared to influence the work reported in this paper.

Acknowledgments

This work was financially supported by the National Natural Science Foundation of China (51673159), the Youth Science and Technology Innovation Team of Sichuan Province of Functional Polymer Composites (2021JDTD0009) and the Sichuan Science and Technology Program (2020YFG0099). SEM characterizations were supported by the Analytical and Testing Center of Southwest Jiaotong University.

References

Aburabie, J., Lalia, B., and Hashaikeh, R. (2021) Proton conductive, low methanol crossover cellulose-based membranes. Membranes 11:539.

Almalki, S.J., and Nadarajah, S. (2014) Modifications of the weibull distribution: a review. Reliab Eng Syst Saf 124:32-55.

Arantes, A.C.C., Silva, L.E., Wood, D.F., Almeida, C.D., Tonoli, G.H.D., de Oliveira, J.E., da Silva, J.P., Williams, T.G., Orts, W.J., and Bianchi, M.L. (2019) Bio-based thin films of cellulose nanofibrils and magnetite for potential application in green electronics. Carbohydr Polym 207:100-107.

Bonardd, S., Moreno-Serna, V., Kortaberria, G., Diaz, D.D., Leiva, A., and Saldias, C. (2019) Dipolar glass polymers containing polarizable groups as dielectric materials for energy storage applications. A Minireview. Polymers 11:317.

Croll, D.C., and Schroeder, L.R. (2004) Synthesis of a ring-rigid disaccharide model for studies of alkaline chain cleavage in cellulose. Journal of Wood Chemistry and Technology 24:27-38.

Cuba-Chiem, L.T., Huynh, L., Ralston, J., and Beattie, D.A. (2008) In situ particle film ATR FTIR spectroscopy of carboxymethyl cellulose adsorption on talc: binding mechanism, pH Effects, and Adsorption Kinetics. Langmuir 24:8036-8044.

Dan, Z.K., Jiang, J.Y., Qian, J.F., Shen, Z.H., Li, M., Nan, C.W., and Shen, Y. (2019) A ferroconcrete-like all-organic nanocomposite exhibiting improved mechanical property, high breakdown strength, and high Energy efficiency. Macromol Mater Eng 304:1900433.

Djahedi, C., Bergenstråhle-Wohlert, M., Berglund, L.A., and Wohlert, J. (2016) Role of hydrogen bonding in cellulose deformation: the leverage effect analyzed by molecular modeling. Cellulose 23:2315-2323.

Fras, L., Johansson, L.S., Stenius, P., Laine, J., Stana-Kleinschek, K., and Ribitsch, V. (2005) Analysis of the oxidation of cellulose fibres by titration and XPS. Colloids and Surfaces A: Physicochemical and Engineering Aspects 260:101-108.

French, A.D. (2014) Idealized powder diffraction patterns for cellulose polymorphs. Cellulose 21:885-896.

He, P., Cao, M.S., Cai, Y.Z., Shu, J.C., Cao, W.Q., and Yuan, J. (2020) Self-assembling flexible 2D carbide MXene film with tunable integrated electron migration and group relaxation toward energy storage and green EMI shielding. Carbon 157:80-89.

Hou, T., Guo, K., Wang, Z., Zhang, X.-F., Feng, Y., He, M., and Yao, J. (2019) Glutaraldehyde and polyvinyl alcohol crosslinked cellulose membranes for efficient methyl orange and Congo red removal. Cellulose 26:5065-5074.

Joyce, D.M., Venkat, N., Ouchen, F., Singh, K.M., Smith, S.R., and Grote, J.G. (2013) DNA hybrid dielectric film devices for energy storage and bioelectronics applications. Paper presented at: Conference on Nanobiosystems-Processing, Characterization, and Applications VI San Diego.

Kaltenbrunner, M., Sekitani, T., Reeder, J., Yokota, T., Kuribara, K., Tokuhara, T., Drack, M., Schwodiauer, R., Graz, I., Bauer-Gogonea, S., et al. (2013) An ultra-lightweight design for imperceptible plastic electronics. Nature 499:458–463.

Lao, J., Xie, H., Shi, Z., Li, G., Li, B., Hu, G.-H., Yang, Q., and Xiong, C. (2018a) Flexible regenerated cellulose/boron nitride nanosheet high-temperature dielectric nanocomposite films with high energy density and breakdown strength. ACS Sustainable Chemistry & Engineering 6:7151-7158.

Lao, J.P., Xie, H.A., Shi, Z.Q., Li, G., Li, B., Hu, G.H., Yang, Q.L., and Xiong, C.X. (2018b) Flexible regenerated cellulose/boron nitride nanosheet high-temperature dielectric nanocomposite films with high energy density and breakdown strength. ACS Sustainable Chemistry & Engineering 6:7151-7158.

Li, Q., Chen, L., Gadinski, M.R., Zhang, S.H., Zhang, G.Z., Li, H.Y., Haque, A., Chen, L.Q., Jackson, T.N., and Wang, Q. (2015) Flexible high-temperature dielectric materials from polymer nanocomposites. Nature 523:576-579.

Li, Q., Yao, F.Z., Liu, Y., Zhang, G.Z., Wang, H., and Wang, Q. (2018) High-temperature dielectric materials for electrical energy storage. In Annual Review of Materials Research, 48:219-243.

Liu, L.M., Qu, J.L., Gu, A.J., and Wang, B.H. (2020) Percolative polymer composites for dielectric capacitors: a brief history, materials, and multilayer interface design. Journal of Materials Chemistry A 8:18515-18537.

Liu, Q.L., Yu, H.T., Mu, T.C., Xue, Z.M., and Xu, F. (2021) Robust superbase-based emerging solvents for highly efficient dissolution of cellulose. Carbohydr Polym 272:118454.

Liu, S.H., Xue, S.X., Zhang, W.Q., Zhai, J.W., and Chen, G.H. (2014) Significantly enhanced dielectric property in PVDF nanocomposites flexible films through a small loading of surface-hydroxylated $Ba_{0.6}Sr_{0.4}TiO_3$ nanotubes. Journal of Materials Chemistry A 2:18040-18046.

Lu, Y., Xie, X., Wang, W.Y., Qi, X.D., Lei, Y.Z., Yang, J.H., and Wang, Y. (2019) ZnO nanoparticles-tailored GO dispersion toward flexible dielectric composites with high relative permittivity, low dielectric loss and high breakdown strength. Composites Part A: Applied Science and Manufacturing 124:105489.

Madusanka, N., Shivareddy, S.G., Eddleston, M.D., Hiralal, P., Oliver, R.A., and Amaratunga, G.A.J. (2017) Dielectric behaviour of montmorillonite/cyanoethylated cellulose nanocomposites. Carbohydr Polym 172:315-321.

Madusanka, N., Shivareddy, S.G., Hiralal, P., Eddleston, M.D., Choi, Y., Oliver, R.A., and Amaratunga, G.A.J. (2016) Nanocomposites of TiO_2/cyanoethylated cellulose with ultra high dielectric constants. Nanotechnology 6:7547-7553.

Moon, R.J., Martini, A., Nairn, J., Simonsen, J., and Youngblood, J. (2011) Cellulose nanomaterials review: structure, properties and nanocomposites. Chemical Society Reviews 40:3941-3994.

Morsi, M.A., Abdelaziz, M., Oraby, A.H., and Mokhles, I. (2019) Structural, optical, thermal, and dielectric properties of polyethylene oxide/carboxymethyl cellulose blend filled with barium titanate. Journal of Physics and Chemistry of Solids 125:103-114.

Movagharnezhad, N., and Moghadam, P.N. (2017) Hexamethylene diamine/carboxymethyl cellulose grafted on magnetic nanoparticles for controlled drug delivery. Polym Bull 74: 4645-4658.

Prateek, Thakur, V.K., and Gupta, R.K. (2016) Recent progress on ferroelectric polymer-based nanocomposites for high energy density capacitors: synthesis, dielectric properties, and future aspects. Chemical Reviews 116:4260-4317.

Sarban, R., Jones, R.W., Mace, B.R., and Rustighi, E. (2011) A tubular dielectric elastomer actuator: Fabrication, characterization and active vibration isolation. Mechanical Systems and Signal Processing 25:2879-2891.

Seddiqi, H., Oliaei, E., Honarkar, H., Jin, J., Geonzon, L.C., Bacabac, R.G., and Klein-Nulend, J. (2021) Cellulose and its derivatives: towards biomedical applications. Cellulose 28:1893-1931.

Takechi, S., Teramoto, Y., and Nishio, Y. (2016) Improvement of dielectric properties of cyanoethyl cellulose via esterification and film stretching. Cellulose 23:765-777.

Tao, J., Cao, S.A., Liu, W., and Deng, Y.L. (2019) Facile preparation of high dielectric flexible films based on titanium dioxide and cellulose nanofibrils. Cellulose 26:6087-6098.

Wang, F.J., Wang, M.H., and Shao, Z.Q. (2018) Dispersion of reduced graphene oxide with montmorillonite for enhancing dielectric properties and thermal stability of cyanoethyl cellulose nanocomposites. Cellulose 25:7143-7152.

Wang, S., Chen, H., Zhou, X., Tian, Y., Lin, C., Wang, W., Zhou, K., Zhang, Y., and Lin, H. (2020) Microplastic abundance, distribution and composition in the mid-west Pacific Ocean. Environmental Pollution 264:114125.

Yang, Q., Zhang, C., Shi, Z., Wang, J., Xiong, C., Saito, T., and Isogai, A. (2018) Luminescent and transparent nanocellulose films containing europium carboxylate groups as flexible dielectric materials. ACS Applied Nano Materials 1:4972-4979.

Yin, Y.N., He, J.C., Zhang, C.G., Chen, J.S., Wu, J.X., Shi, Z.Q., Xiong, C.X., and Yang, Q.L. (2021) Flexible cellulose/alumina (Al_2O_3) nanocomposite films with enhanced energy density and efficiency for dielectric capacitors. Cellulose 28:1541-1553.

Yin, Y.N., Zhang, C.G., Yu, W.C., Kang, G.H., Yang, Q.L., Shi, Z.Q., and Xiong, C.X. (2020) Transparent and flexible cellulose dielectric films with high breakdown strength and energy density. Energy Storage Mater 26:105-111.

Yu, H., Duan, J., Du, W., Xue, S., and Sun, J. (2017) China's energy storage industry: Develop status, existing problems and countermeasures. Renewable & Sustainable Energy Reviews 71:767-784.

599 Yuan, M.X., Zhang, G., Li, B., Chung, T.C.M., Rajagopalan, R., and Lanagan, M.T. (2020) Thermally
600 stable low-loss polymer dielectrics enabled by attaching cross-linkable antioxidant to
601 polypropylene. Acs Applied Materials & Interfaces 12:14154-14164.
602 Zeng, X., Deng, L., Yao, Y., Sun, R., Xu, J., and Wong, C. P. (2016) Flexible dielectric papers based on
603 biodegradable cellulose nanofibers and carbon nanotubes for dielectric energy storage.
604 Journal of Materials Chemistry C 4:6037-6044.
605 Zhang, C., Li, P.P., Zhang, Y.J., Lu, F., Li, W.W., Kang, H.L., Xiang, J.F., Huang, Y., and Liu, R.G.
606 (2016) Hierarchical porous structures in cellulose: NMR relaxometry approach. Polymer 98:
607 237-243.
608 Zhang, C.G., Yin, Y.N., Yang, Q.L., Shi, Z.Q., Hu, G.H., and Xiong, C.X. (2019) Flexible
609 Cellulose/BaTiO3 Nanocomposites with High Energy Density for Film Dielectric Capacitor.
610 Acs Sustainable Chemistry & Engineering 7:10641-10648.
611 Zhang, X., Zhang, Y., Zhou, Q., Zhang, X.L., and Guo, S.Y. (2020) Symmetrical "sandwich"
612 polybutadiene film with high-frequency low dielectric constants, ultralow dielectric loss, and
613 high adhesive strength. Industrial & Engineering Chemistry Research 59:1142-1150.
614 Zhao, D., Huang, J.C., Zhong, Y., Li, K., Zhang, L.N., and Cai, J. (2016) High-strength and high-
615 toughness double-cross-linked cellulose hydrogels: A new strategy using sequential chemical
616 and physical cross-linking. Adv Funct Mater 26:6279-6287.
617 Zhao, D.W., Zhu, Y., Cheng, W.K., Chen, W.S., Wu, Y.Q., and Yu, H.P. (2021) Cellulose-based flexible
618 functional materials for emerging intelligent electronics. Advanced Materials 33:2000619.
619 Zhao, Y.H., Guo, Q.W., Wu, S., Meng, G., and Zhang, W.M. (2019) Design and experimental validation
620 of an annular dielectric elastomer actuator for active vibration isolation. Mechanical Systems
621 and Signal Processing 134:106367.
622 Zheng, W., and Wong, S.C. (2003) Electrical conductivity and dielectric properties of
623 PMMA/expanded graphite composites. Composites Science and Technology 63:225-235.
624